Conceptual Model of Expansive Rock or Soil Swelling

Kavur, Boris; Štambuk Cvitanović, Nataša Štambuk; Jug, Jasmin; Vrkljan, Ivan

geosciences

IMPACT FACTOR 2.7

CITESCORE 5.2

Article

Conceptual Model of Expansive Rock or Soil Swelling

Boris Kavur, Nataša Štambuk Cvitanović, Jasmin Jug and Ivan Vrkljan

Topic

Support Theory and Technology of Geotechnical Engineering

Edited by

Prof. Dr. Qi Wang, Dr. Bei Jiang, Dr. Xuezhen Wu and Dr. Hongke Gao

MDPI

https://doi.org/10.3390/geosciences13050141

geosciences

MDPI

Article

Conceptual Model of Expansive Rock or Soil Swelling

Boris Kavur [1,*], Nataša Štambuk Cvitanović [2], Jasmin Jug [1] and Ivan Vrkljan [3]

[1] Faculty of Geotechnical Engineering, University of Zagreb, Hallerova Aleja 7, 42000 Varaždin, Croatia; jasmin.jug@gfv.unizg.hr
[2] Faculty of Civil Engineering, Architecture and Geodesy, University of Split, Matice Hrvatske 15, 21000 Split, Croatia; nstambuk@gradst.hr
[3] Faculty of Civil Engineering, University of Rijeka, Radmile Matejčić 3, 51000 Rijeka, Croatia; ivan.vrkljan@gradri.uniri.hr
* Correspondence: boris.kavur@gfv.unizg.hr

Abstract: The paper presents a simple yet efficient way to track the void ratio, the water content, and the degree of saturation of a swelling material during saturation. The research aimed to quantitatively describe the drying and wetting processes of the swelling material, which should enable their better understanding and easier modelling. Two identical tall samples, named "twins", were formed by consolidating the paste prepared from the swelling material in which montmorillonite is the dominant mineral. The twins were together exposed to one-dimensional drying. After drying, lasting for 40 days, one twin was dissected to determine its water content profile. The other twin was subjected to 1D wetting (ponded infiltration experiment) with a constant water column for a period of 21 days and then dissected to determine the moisture profile. The sample preparation reduces uncertainties about the initial state. The results show that during wetting, the material follows a path in the e-w plot which is parallel to the full saturation curve. After reaching some degree of saturation, the path becomes parallel to the residual (shrinking) line. The proposed model predicts the primary and secondary phases of swelling, and under appropriate conditions, it assumes the tertiary phase.

Keywords: swelling rock and soil; shrinkage curve; swelling curve; model of swelling; ponded infiltration experiment

Citation: Kavur, B.; Štambuk Cvitanović, N.; Jug, J.; Vrkljan, I. Conceptual Model of Expansive Rock or Soil Swelling. *Geosciences* **2023**, *13*, 141. https://doi.org/10.3390/geosciences13050141

Academic Editors: Jesus Martinez-Frias and Mohamed Shahin

Received: 2 March 2023
Revised: 25 April 2023
Accepted: 7 May 2023
Published: 11 May 2023

1. Introduction

Expansive rocks and soils expand in volume when exposed to wetting and decrease their volume when losing water. Such rocks or soils create serious problems for construction if structures are built in (tunnels e.g., [1,2]) or on top of them (foundations). However, there are countless examples of tunnel damage or serious damage to entire settlements and roads built on expansive material. Swell–shrink rocks or soils are one of the most frequent and costly global geological hazards. Numerous studies of such hazards have been carried out [3–10]. Therefore, for rational design in such conditions, it is necessary to have a good understanding of the mechanisms that lead to changes in volume and to have the possibility of realistic forecasting of the behaviour of the expansive material during construction and later during the use of the building.

Swelling rocks and soils are composed of a mixture of minerals, among which smectites have the most important influence on swelling and shrinkage. Montmorillonite belongs to the smectite group of clay minerals. The main characteristic of these minerals is their high affinity toward water molecules, and they increase their volume by binding with water. The microstructure is formed by clusters of unit particles of the montmorillonite mineral dominated by interlayer pore spaces and micropores between individual particles. The microstructure is part of the material's macrostructure, consisting of clusters of particles with macropores. Physicochemical actions within the microdomain and macrodomain determine the behaviour of the expansive material during drying and wetting [11].

It has been observed that a natural material with a high swelling potential, if it is completely saturated, will not swell when submerged or exposed to water [12]. Indeed, the swelling potential will only be activated if the material is desaturated in a certain way. Desaturation in natural conditions usually occurs due to drying or evaporating pore water. Drying is a natural phenomenon during the construction of any building, whether it involves surface or underground excavations or the use of expansive material as a barrier to prevent water seepage in landfills.

Investigations of drying and wetting of swelling rocks were carried out at the level of a laboratory sample. Samples of the swelling rock from Muvrinski Jarak near Popovača (Croatia) were used.

The research program that preceded this included the experimental determination of the characteristic hydraulic functions of the swelling rock material [13] necessary for the quantitative description of the drying and wetting processes. The hydraulic properties of the swelling rock were determined using the test procedures developed at the University of Colorado in Boulder [14–21]. These test procedures provided the soil–water retention curve (SWRC) and the function of hydraulic conductivity in saturated and unsaturated conditions.

The main goals of this research were to quantitatively describe the drying and wetting processes of the swelling material, which should enable a better understanding of its behaviour and easier modelling, and to explore the hysteresis between drying and wetting paths, which is poorly understood due to a lack of research in this regard [22].

To carry out the planned tests, a special and carefully designed procedure and equipment were used to prepare two identical tall cylindrical samples, so-called twins. The twins were prepared by consolidating a paste of swelling material in a tall cylinder rather than by the compaction process commonly used to prepare test specimens in similar trials. The preparation of tall samples was technically demanding and time-consuming. The goal of the preparation was to make samples of swelling material with a homogeneous structure and uniformly distributed humidity, which were almost saturated at the beginning of the test. Tall samples should enable monitoring of the 1D drying process (the upper surface of the sample is exposed to drying) and then 1D wetting along the depth of the swelling material. Measurements of diameter changes along the height of tall samples will allow for monitoring of the progress of the drying and wetting fronts during tests. It is important to emphasize that the samples' drying process starts from a clearly defined initial state of humidity, void ratio, and saturation. After 1D drying, one sample was subjected to 1D wetting with a constant column of water from the top surface. Before its wetting, the state of humidity, void ratio, and saturation of the dried sample were determined by testing one of the twin samples. Monitoring the changes along the depth of the material is particularly important for the analysis of the 1D wetting process when the wetting front advances downward. According to the results of experiments conducted by Garnier et al. [23], and also according to previous tests conducted by Kavur [24], it was observed that the swelling material at the surface behaves differently from the material at a depth.

The idea of this research was to start the experiments of drying and wetting from clearly defined initial conditions of humidity, void ratio, and saturation, which will allow us to quantitatively describe the drying and wetting processes by appropriate measurements of changes in the mass and volume of the samples so that they can then be appropriately analyzed.

2. Shrinkage Curve

The problems of swelling and shrinkage are closely related to climatic conditions, so the problem is most pronounced in regions with an arid and semi-arid climate. The change in the volume of the expansive material includes the phenomenon of water flow in an unsaturated, deformable, porous medium. A rational solution to such a problem requires defining the characteristic hydraulic curves of the expansive material: the soil–water retention curve (SWRC) or soil–water characteristic curve [25], the hydraulic conductivity function, and the curve of the relationship between the volume and the proportion of water in the swelling material (shrinkage–swelling curve). Despite this, swelling forecasts

based on the suction variable have not been widely used due to known difficulties in measuring suction and problems in experimentally determining the hydraulic conductivity of unsaturated media [26].

The behaviour of the swelling rock during drying can be shown by the shrinkage curve (Figure 1), which represents the relationship between the change in volume or the void ratio and the water content. The curve in Figure 1 shows two phases of volume shrinkage, and, in general, it can have up to four different phases during drying [27].

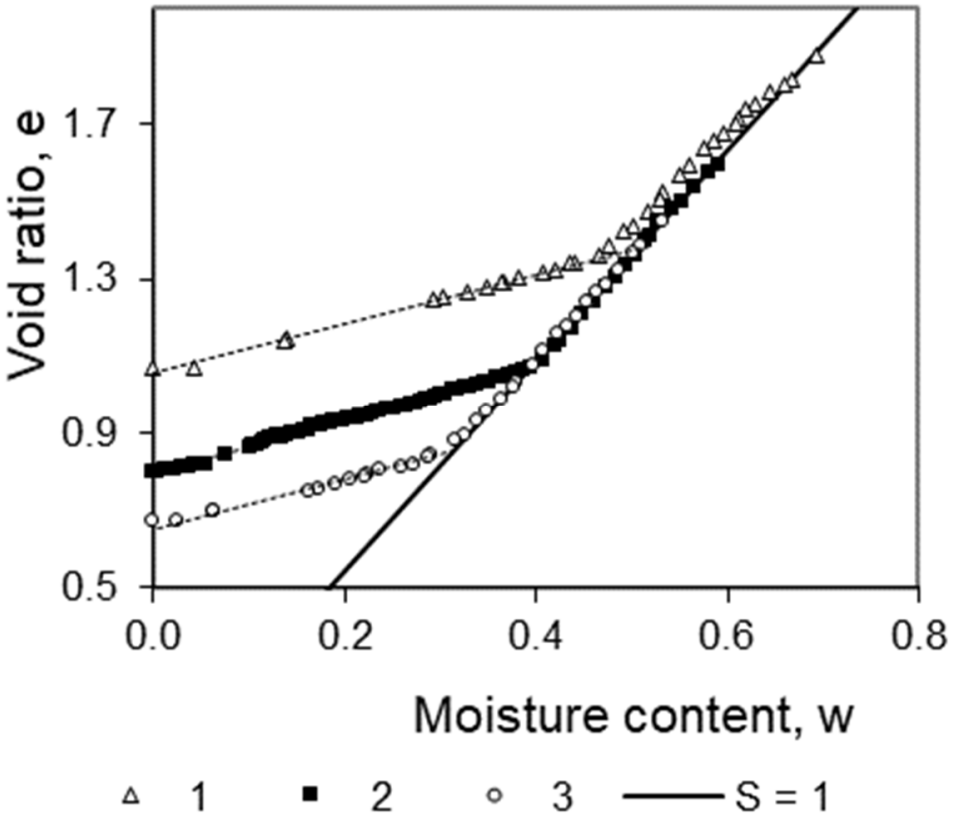

Figure 1. Shrinkage curves determined for reconstituted samples that were consolidated at different vertical loads: 1, 800 kPa; 2, 1600 kPa; 3, 3200 kPa [28].

The magnitude of the volume shrinkage due to the increase in total suction depends on the stiffness of the structure of the swelling material, which in turn depends on numerous factors: stress history, the proportion of active clay minerals and other minerals in the material, the possible existence of mineral bonds (except clay minerals) within the structure, etc.

The swelling material at the beginning of drying may show volume changes corresponding to the volume of evaporated water. Despite water losses, the material remains at the same degree of saturation [29]. The volume change equals the volume of evaporated water up to the point where air penetration occurs. We call this phase the proportional shrinkage phase. The volume of any gas phase present during the proportional phase remains constant [27,30].

When the suction reaches a value sufficient for air to enter the pores of the swelling material, which depends on the pore size, the volume changes become smaller than the volume of evaporated water, and the degree of saturation decreases (unsaturated state) with water loss. We call this phase the phase of residual shrinkage. In general, proportional and residual shrinkage phases dominate the drying process because they are where the most significant changes in volume and moisture are realized.

In addition to the proportional and residual phases, in some cases, the swelling material can also show a phase of structural contraction at the beginning of drying. In that phase, the volume change is smaller than the volume of evaporated water. The phase

of structural shrinkage is followed by the phase of proportional or immediate residual shrinkage. At the end of drying, in some cases, the so-called zero shrinkage phase occurs after the reduction in volume reaches the material's shrinkage limit when, despite drying and an increase in suction magnitude, there is no further change in volume. In structural and residual shrinkage phases, volume changes are smaller than the volume of lost water.

The shrinkage curve is usually determined on an unloaded sample, which, during drying, is affected only by changes in the suction variable due to changes in water content. However, in actual conditions, the effect of the normal stress variable due to the weight of the overlay sediments should be considered, as well as the possible effect of some additional external load on the surface.

Raats [31] states that probably the best set of shrinkage curves at different vertical stresses is published by Talsma [32]. Talsma investigated the shrinkage of clay paste samples during drying exposed to different vertical loads. At a constant value of the vertical load, the samples were gradually desaturated by drying. As a result, the shrinkage curves obtained at different values of vertical load were practically parallel.

In previous studies [24], several series of natural, undisturbed test samples with different initial densities and water content formed from larger pieces of swelling rock were subjected to drying experiments. The initial dry density of these samples ranged widely from 0.92 to 1.19 Mg/m^3, and the void ratio ranged from approximately 1.29 to 1.97. The research showed that the obtained shrinkage curves are parallel to each other despite the significantly different initial states of dry density and moisture content of the tested samples. From tests on the reconstituted samples, parallel shrinkage curves were also obtained in a wide range of normal loads, from 800 to 3200 kPa (Figure 1).

By researching the literature [27,29,32–39] and based on the behaviour observed here, it is concluded that the slope of the residual part of the shrinkage curve represents a specific characteristic of the swelling material. The slope of this part of the shrinkage curve does not change with the degree of over-consolidation.

Numerous recent studies investigated the shrinkage and swelling of soils and desiccation cracking [40–49].

3. Conceptual Model of Swelling

Wetting test models of swelling material, e.g., [50,51], commonly interpret volume changes by assuming a unique swelling curve (identified with a shrinkage curve) in wetting or starting infiltration at uniformly distributed moisture throughout the depth of the sample, which facilitates interpretation and does not give an accurate picture of this problem. Three-dimensional changes in the volume of swelling material can be represented by a simple model [50–57], which simultaneously includes vertical and lateral isotropic deformation of the skeleton (solid phase).

While the shrinkage curve can be determined relatively easily by experimenting with drying a deformable–expansive material (Figure 1), determining the swelling curve during wetting is very demanding. Namely, wetting such a material with a low moisture content is a dynamic and transient process that simultaneously involves sudden changes in the volume and water content of the material where the usual mass and volume measurement techniques are not readily applicable. For this reason, some researchers used the gamma-ray attenuation measurement technique [50,58,59]. The problem with classical gamma binary sources is the relatively weak energy intensity and long measurement time [23].

It is most often assumed that the swelling curve is identical to the shrinkage curve or that the hysteresis between drying and wetting paths is ignored. That is why complex drying and wetting processes are simplified.

A recent study carried out by Onyelowe et al. [22], which examined 403 relevant literature references studying the utilization of soil–water retention curve as a tool in solving most geotechnical engineering problems, reached the following conclusion: "Hydraulic hysteresis is a fundamental issue in unsaturated soil that makes the difference between drying and wetting paths in the soil-water retention curve. The causes of this phenomenon

are still a question despite some previous investigation on this topic". These facts justify the efforts made in this research to shed light on the hysteresis problem between the drying and wetting of swelling materials.

The existence of hysteresis in the soil–water retention curve [60–63] indicates that we should also expect hysteresis between the shrinkage and the swelling curves here. Namely, due to the hysteresis in the soil–water retention curve, the suction value during wetting is lower than the suction value during drying, with the same water content. This means that during wetting with the same water content, the value of the void ratio should be higher than during drying. The mechanical behaviour of swelling soil in terms of volume change is also accompanied by microstructural changes in fabric and structure [64].

Yong [65] developed a theoretical model explaining the interaction between a swelling material's micro- and macro-structural elements. It was used to explain the observed behaviour of swelling rocks [11] and to develop the conceptual model of the swelling curve in this study. Interlayer spaces and micropores form a microstructure that is part of the swelling material's macrostructure, consisting of aggregates of clay particles with macropores located between adjacent aggregates of unit particles. The microstructure's absorption and water retention properties differ significantly from the macropores.

Figure 2 shows the conceptual model of the swelling curve, i.e., the behaviour model of the representative elementary volume (REV) of the swelling material in the wetting process. The diagram in Figure 2 shows the relationship between the void ratio (e) and the moisture coefficient (ϑ). The moisture coefficient is defined as the quotient of the volume of water and the volume of solid particles of the swelling material. For modelling the water flow in an expansive media, it is more appropriate to use the moisture coefficient variable than the volumetric water content because the volume of the expansive material varies during water flow.

The swelling curve, shown in Figure 2, is divided into primary and secondary phases by the concept proposed here, and, under appropriate conditions, the concept also includes the tertiary swelling phase. During wetting, an increase in the moisture content of the swelling material means a decrease in the suction value, an increase in the hydraulic conductivity, and an increase in the void ratio.

Let us assume the swelling material is significantly dried before wetting, i.e., point (eo;ϑo) in Figure 2. That is, we assume a significant water deficit in the REV microstructure. In the total suction at the beginning of wetting, the contribution of microstructural pore spaces dominates. The contribution of macropores to the total suction in this phase is negligible compared to the action of the microstructure. For this reason, water movement at the beginning of wetting is exclusively directed toward the microstructural spaces [65]. Water movement occurs as a thin film at the boundaries of particles or aggregates, not in large pore spaces. The swelling concept proposed here assumes that the volume change in the REV in the primary phase can reach the value of the volume of infiltrated water. We will call this phase the primary swelling phase. The concept assumes that the swelling curve in the primary phase is parallel to the swelling material's full saturation direction.

The entry of water into the microstructural elements leads to a gradual decrease in the overall suction of the REV. By weakening the gradients in the microstructural pore spaces, the gradual access of water into the macropores is enabled. The water distribution is determined by the mutual relationship between the microstructural elements' osmotic potential and the clusters' matric potential [65]. Due to the possibility of water entering the macropores in this swelling phase, volume changes are smaller compared to the primary phase. Therefore, we will call this phase the secondary swelling phase.

The proposed swelling concept is based on the important fact that the slope of the secondary part of the swelling curve is approximately equal to the slope of the shrinkage curve in the residual phase. This fact was discovered and confirmed by previous research on the gradual wetting of small disc-shaped samples [24]. The suction magnitude gradually weakens during wetting compared to the magnitude during the drying process. Research carried out by Talsma [32] and the curves shown in Figure 1 in this research clearly show

the effect of the reduced magnitude of load or suction. Based on this, it is logical to expect that the shrinkage curves in the residual drying and the swelling curves in the secondary swelling phases would be parallel because they refer to the same pore spaces.

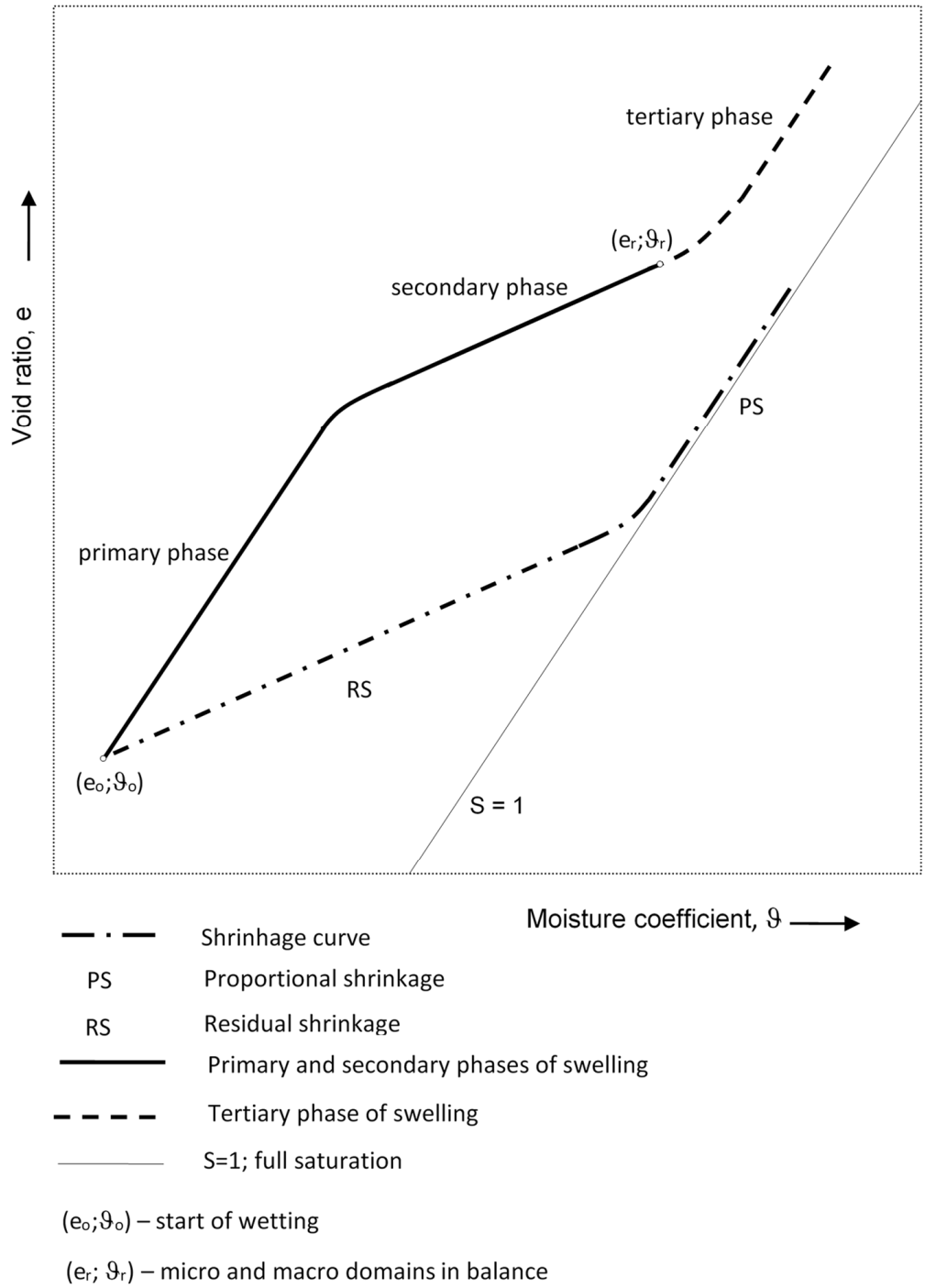

Figure 2. Swelling phases of the representative elementary volume (REV).

During secondary swelling, there is a further drop in suction in the microstructure. Part of the air remains permanently trapped inside the macropores. The action of the osmotic potential in the microstructure is exposed to the counteraction of the matrix potential of the macrostructure. Yong [65] assumes that in the equilibrium state, i.e., point (er;ϑr) in Figure 2, water absorption in the microstructural spaces is stopped by the existence of matrix sorption forces demonstrated by aggregates, and, thus, the wetting and swelling

process is stopped. At the same time, the microstructural spaces are completely saturated, while the macrostructure of the REV remains partially unsaturated.

Suppose that the balance of the opposite effects of suction between the macro- and microdomains is not established. In that case, the swelling process due to the osmotic potential in the microstructure can continue. We will call this phase, which is indicated by a dashed line in the continuation of the swelling curve (Figure 2), the tertiary swelling phase.

The proposed model assumed that the conditions for the formation of the tertiary phase of swelling could occur in more dried material in the so-called free swelling, that is, when there is no significant obstruction to the expansion of the volume of the swelling material and when wetting is carried out with an abundant (sufficient) amount of water. Such conditions appear in the shallow surface part of the swelling material. The structure of the material here is cracked during drying due to the action of high tensile stresses. The microstructure has a significant water deficit, and the material swells rapidly. Moreover, the hydraulic conductivity is very low. The surface-moistened layers, located above the still-dry, lower-lying material, intensively absorb water and, as such, increase in volume. Finally, the aforementioned leads to shear stresses in the plane of the wet front.

With increasing water content and swelling, van der Waals's attractive forces suddenly weaken, while repulsive electric forces (the phenomenon of the electric double layer), on the contrary, unexpectedly strengthen. The consequence of such a development of changes in the action of attractive and repulsive forces is a sudden weakening and breaking of cohesive bonds within the REV structure. Due to the disintegration of the structure, the osmotic action does not encounter obstruction in the form of matrix action from the macrodomain. That is, the balance is not established as previously described. The swelling in these conditions ends only after the dissipation of the suction in the micro spaces or after the eventual establishment of a balance between the osmotic action in the microdomain and the forces that resist the volume change. The described actions cause a very intense and rapid change in volume and the disintegration of the structure of the swelling material during the tertiary phase of swelling.

The hypothesis presented here about the existence of three different phases of swelling came from the analysis of the results of the wetting experiment of a swelling material sample, which is elaborated on in the fifth chapter here, and the analysis of the results of the wetting of the Vertisol sample conducted by Garnier et al. [23]. Based on these results, it is assumed that the tertiary part of the swelling curve is approximately parallel to the line of full saturation or that it tends to reach full saturation at a relatively high void ratio and water content (Figure 2).

Within the hypothesis of the existence of different stages of swelling, it is further concluded that the swelling curve is not a unique one for all swelling material affected by the wetting process, as is the shrinkage curve in drying, but that the discrete parts of the swelling model have separate curves that start from their initial water contents at the beginning of wetting (the arrival of a wet front). It is also assumed that their curves, or parts of the curves that correspond to the described stages of swelling, are parallel.

Garnier et al. [23] used the so-called synchrotron dual X-ray source with a much stronger intensity and sharpness than gamma sources, and the measurement process is 200 times faster at the same level of accuracy. With this technique, it is possible to simultaneously measure the density of solid particles and the water content of the porous medium. In addition, they performed density and water content measurements in the initial wetting phase of a bentonite–sand mixture and a Vertisol swelling soil sample.

The behaviour of the Vertisol sample, prepared as a prism, with a cross-section of 4×4 cm and an initial height of 6.2 cm, is very similar to the behaviour of the "twin" in this research. The authors emphasize that the material on the top of the Vertisol sample with a thickness of about 1 cm behaves differently from the rest. That is, the material on the top disperses in water. From the measured curves of changes in density and volumetric water content registered in the initial phase of wetting [23], swelling curves were calculated here for the thin layers of the Vertisol sample (Figure 3) located below the surface layer dispersed

in water. The phases can be clearly identified on the calculated curves (Figure 3), called the primary and secondary swelling phases. A secondary phase explains the apparent discrepancy between the infiltration curve and the volume change curve of the Vertisol sample. Namely, the infiltration curve shows a constant increase in the amount of infiltrated water, while the volume change curve simultaneously has a practically constant value.

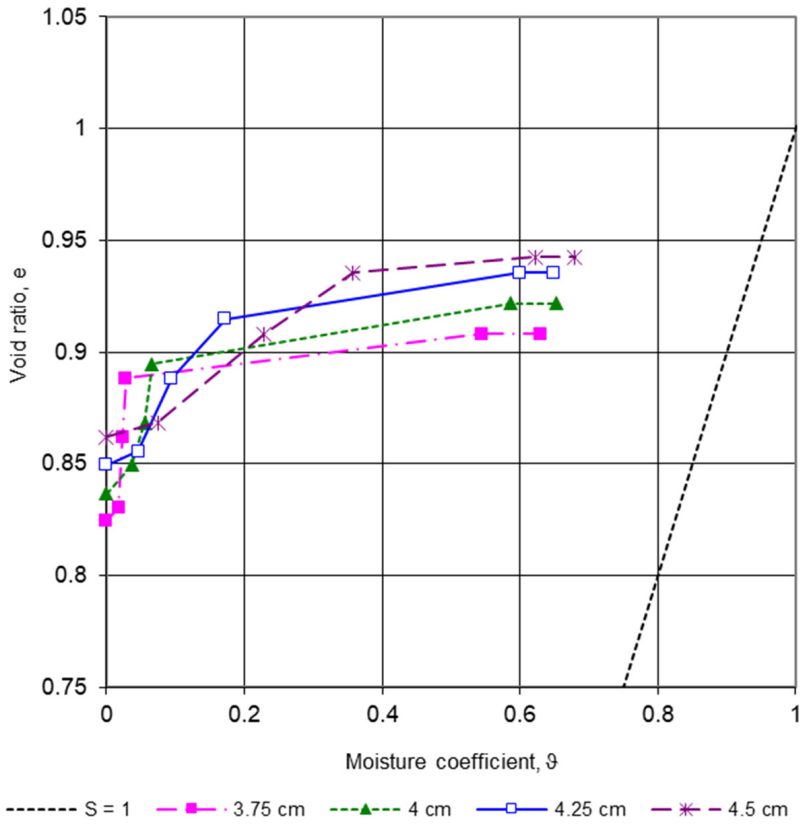

Figure 3. Reinterpretation of the results of the wetting test of a Vertisol sample with an initial height of 6.2 cm, performed by Garnier et al. [23] (swelling curves interpreted at different levels of the test sample during the wetting test).

4. Material and Test Procedures

Investigations of drying and wetting the swelling material were carried out at the level of a laboratory sample. Swelling rock samples from the Muvrinski Jarak locality in the wider area of the Gornja Jelenska near Popovača (Croatia) were used. The plasticity index of the selected material was around 54%, and the liquid limit ranged from 99 to 112%. In the natural state, the proportion of water ranged in a very wide range of 45 to 71%, and the void ratio was from 1.29 to 1.97. Mineralogical analyses showed that montmorillonite was the dominant clay mineral in the selected samples.

Previous tests of the same swelling material were performed to determine the following characteristic hydraulic functions, which are necessary for the quantitative description of drying and wetting processes [13,24,28,66]: the soil–water retention curve (SWRC), which represents the relationship between suction and moisture content of the material, the hydraulic conductivity curve (HCC) in saturated and unsaturated conditions, and the soil shrinkage curve (SSC) of the material during drying.

Wetting and swelling tests of such materials are usually performed on unsaturated, compacted samples where the initial state is unclear. Therefore, these tests were started here by drying from a clearly defined initial state and monitoring humidity and volume changes. At the end of drying, the sample's state before wetting and swelling was clearly defined.

For research at the laboratory sample level, the samples must have a homogeneous composition and structure so that possible local irregularities in the material's composition

and/or structure do not significantly impact the test result. For example, the natural swelling rock shows the sporadic appearance of isolated, smaller, and larger inclusions of sand, concretions, and other formations up to several centimeters in diameter. The influence of such sporadic, isolated phenomena or minor irregularities within the basic structure of the swelling material on its behaviour in drying and wetting conditions is very limited and can be ignored. However, at the level of a laboratory sample, such phenomena can have a significant impact on test results, and they can distort the picture of the behaviour of the basic material. Since it was impossible to observe or avoid these isolated phenomena during the formation and preparation of undisturbed test samples, we resorted to preparing homogeneous, reconstituted samples from the basic swelling material.

The reconstituted samples were formed by the consolidation of paste with high initial moisture content. The swelling material was previously dried and then crushed in a mortar to prepare these samples. The crushed material was sieved in a sieve with an opening size of 0.425 mm. The material fraction that passed through the sieve was mixed with deaerated, distilled water into a suspension paste with an initial water content of about 200%. In the tests that preceded these [24], disc-shaped test samples were prepared by consolidating the paste into specially designed oedometer cells. The test samples for the tests that are the subject of this paper were prepared in the same way as previous consolidations, but this time in a specially constructed cylinder (Figure 4a–c) to obtain tall cylindrical samples (Figure 4d–f) of swelling material for 1D drying and 1D wetting experiments. At the end of the consolidation process and after gradual unloading, tall cylindrical samples were left in distilled water until complete relaxation. This preparation aimed to obtain fully saturated and homogeneous samples of swelling material.

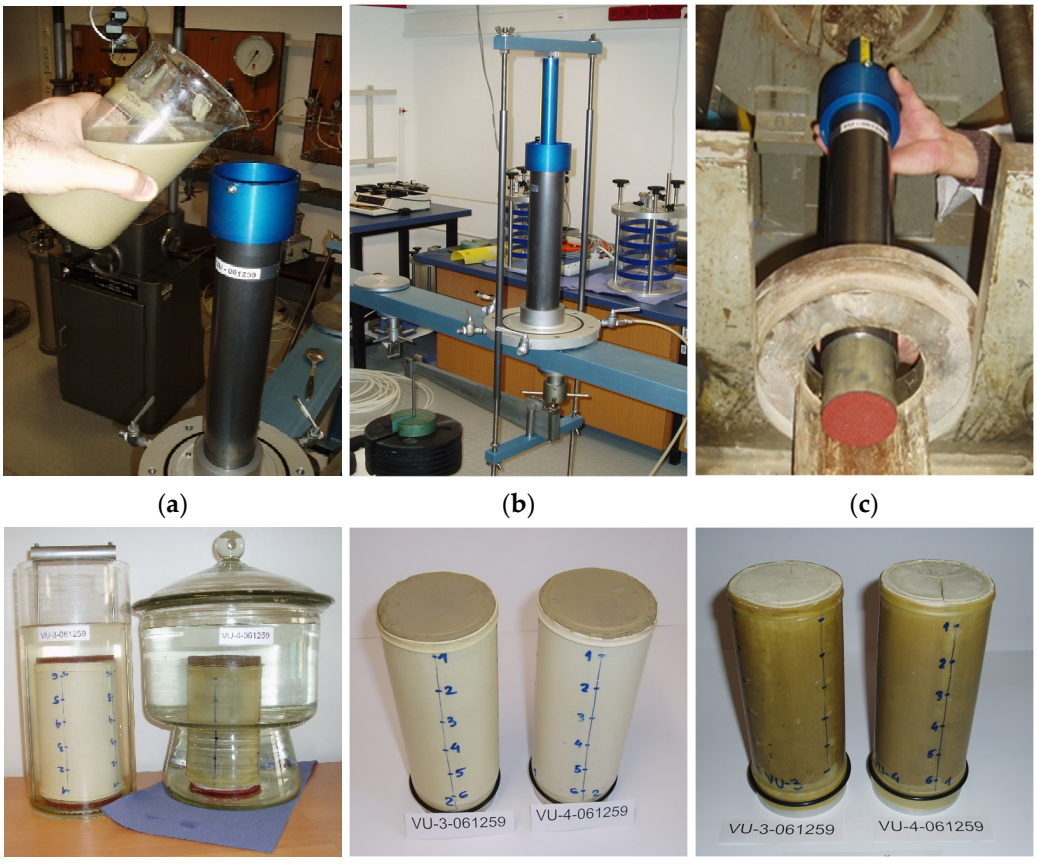

(**a**) (**b**) (**c**)

(**d**) (**e**) (**f**)

Figure 4. Stages of preparation (**a**–**c**); relaxation in water (**d**), and 1D drying (**e**,**f**) of the twins.

Tall, reconstituted samples were subjected to one-dimensional drying and wetting tests to provide data on changes in sample mass, drying and wetting speed, height and diameter (measured along the sample height at predefined sections), volume during shrinkage and swelling, and moisture distribution per depth of swelling material. The way samples were prepared ensured that their initial state of saturation, water content, and void ratio distribution within the material was clearly defined at the beginning of the test. Thus, during drying and wetting tests, the changes in humidity and volume of the samples exposed to 1D drying and then 1D wetting according to the planned program could be monitored with appropriate measurements.

Two identical tall samples, named "twins", were formed by consolidating the paste in a tall cylinder (Figure 4d–f). Side by side in the laboratory, these samples were, at the same time, exposed to one-dimensional drying under identical environmental conditions. The assumption was that such samples should behave identically during drying and that the humidity distribution in the material's depth in both samples would be identical. After drying, one twin was cut into disks to measure the moisture profile along the depth of the material, and the other twin was subjected to one-dimensional wetting. The initial state, i.e., the saturation, water content, and void ratio profiles in the sample subjected to wetting, were determined by testing the first twin.

The bottom of a standard triaxial cell (for testing soil samples with a diameter of 70 mm) was used as a cylinder base for paste consolidation. The cylinder's inner diameter corresponded to the sample stand's diameter. The diameter of the piston was about 0.1 mm smaller than the diameter of the cylinder, and rubber o-rings on the piston and the sample stand additionally ensured water tightness along the cylinder walls. The twins were gradually consolidated to a vertical load of 1600 kPa. After unloading and resting in water, the twins prepared in this way had appropriate strength and stiffness to enable the planned manipulations and testing operations.

The successful preparation of the twins, two identical samples with the laboratory markings VU-3 and VU-4, was preceded by the preparation of three tall samples on which sufficient experience was gained. At the same time, some errors that were found in the construction of the device, as well as in the preparation procedure, were eliminated.

Immediately after removing from the cylinder and measuring the height and weight of the samples, the samples were immersed in distilled water (Figure 4d) for complete relaxation and preservation of saturation before the start of the drying tests.

Data related to the preparation of the twins are presented in detail in [24]. Before drying, the twins were at a wet density $\rho = 1.65$ g/cm^3, a void ratio $e = 1.60$, a water content $w = 0.58$, and a degree of saturation $S = 0.99$.

5. Test Results

5.1. Drying of Twins (VU-3 and VU-4)

Before drying, the twins are divided by height with markings (virtually) into six discs of equal height (Figure 4e,f). Using a digital caliper, a mark (measuring point) was placed in the middle of each disk to measure changes in diameter during drying. Changes in diameter were measured in two perpendicular directions. The diameters of each disc were measured before and after placing a protective rubber membrane on the sample's sheath, which prevented lateral humidity changes. During drying, only the upper surface of the twin was exposed to air in the laboratory, where changes in temperature and air humidity near the twins were continuously measured and registered. A rubber ring over the sample stand secured the membrane. The airflow speed at the drying place was negligibly low. The twins were, thus, simultaneously, side by side, subjected to one-dimensional drying in the laboratory under identical environmental conditions.

The twins were exposed to drying for 40 (VU-4) and 41 days (VU-3), respectively. Mass changes, rate of water loss during drying, and volume changes in both samples were very similar—almost identical. The curves of changes in the mass of the twins during drying are shown in Figure 5.

After 40 days of drying, the VU-4 twin was freed from the membrane. The heights of the discs between the set marks were measured, and the diameters of each disc without the membrane were measured.

The VU-4 twin was then divided into 12 discs of equal height by engraving new markings. At the middle of the height of each disc, the diameter was measured in two perpendicular directions. The sample was cut into discs according to the engraved marks. During cutting, the discs fell apart. The moisture content of the material of each disc was determined (Table 1) after drying in a drying oven at 60 °C. The disc from the bottom of the sample was saved by carefully cutting off the material. With this disk, the moisture content and the material's void ratio at the end of drying was determined. The final porosity, i.e., the void ratio corresponding to the material's shrinkage limit (e_o = 0.84), was also determined. Finally, the void ratios of all other discs were determined based on knowledge of the relationship between the void ratio and moisture content in the residual phase ($e = 0.66w + 0.84$) and the measured moisture content (Table 1).

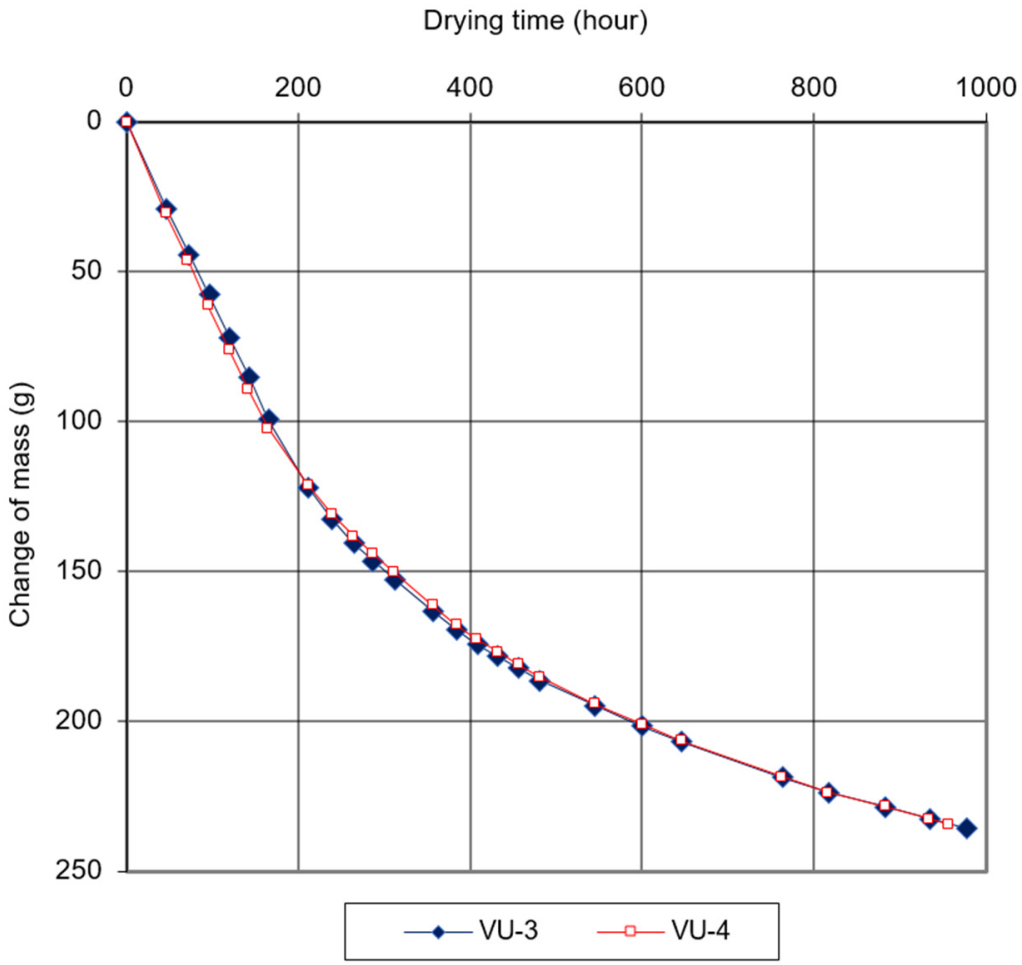

Figure 5. Mass loss of samples (twins) during drying in the laboratory.

Table 1. Conditions of sample VU-4 after drying for 40 days.

After drying for 40 days, sample VU-4-was divided into 12 discs of equal height: 12.15 mm. Discs no. 1 to 10 were physically divided by cutting. During cutting, the material broke into pieces of irregular shapes. Discs no. 11 and 12 (bottom of the column) were not divided to preserve the integrity of that part of the sample. The preserved bottom of the sample made it possible to measure the volume before and after drying in a drying oven at 60 °C. Based on this, the following were determined: the void ratio (e) at the moisture content (w) found after drying, the shrinkage limit of the material (e_o), and the slope of the residual shrinkage phase curve (k_{rez}).
At moisture content w = 0.289, the measured void ratio is e = 1.03. After drying in a drying oven at 60 °C to a constant mass, the void ratio (shrinkage limit) is e_o = 0.84. The slope of the residual phase direction of the volume shrinkage $k_{rez} = \frac{e-e_o}{w-w_o} = 0.66$.
Specific gravity of solid particles: 2.72
Relation between moisture content and void ratio: for $w > 0.408 \rightarrow e = 2.72\ w \rightarrow$ proportional shrinkage phase for $w < 0.408 \rightarrow$ e = 0.66 w + 0.84 $\rightarrow$ residual shrinkage phase

VU-4	Measured					Calculated					
Disc no.	H. of meas. point (mm)	Disc diam. (mm)	Disc volume (cm^3)	Moisture content, w	Void ratio, e	Void volume (cm^3)	Volume of solids (cm^3)	Water mass (g)	Mass of solids (g)	Disc mass (g)	Degree of saturation, S
1	139.7	66.10	41.7	0.079	0.89	19.7	22.0	4.76	59.92	64.68	0.24
2	127.6	66.13	41.7	0.130	0.93	20.1	21.7	7.64	58.94	66.58	0.38
3	115.4	66.37	42.0	0.177	0.96	20.5	21.5	10.32	58.43	68.75	0.50
4	103.3	66.66	42.4	0.215	0.98	21.0	21.4	12.49	58.19	70.69	0.59
5	91.1	66.84	42.6	0.240	1.00	21.3	21.3	13.93	58.02	71.95	0.65
6	79.0	67.04	42.9	0.259	1.01	21.6	21.3	15.03	58.00	73.03	0.70
7	66.8	67.10	43.0	0.271	1.02	21.7	21.3	15.66	57.89	73.55	0.72
8	54.7	67.09	42.9	0.279	1.02	21.7	21.2	16.09	57.71	73.80	0.74
9	42.5	67.10	43.0	0.285	1.03	21.8	21.2	16.41	57.62	74.02	0.75
10	30.4	67.12	43.0	0.289	1.03	21.8	21.2	16.64	57.57	74.21	0.76
11	18.2	67.10	43.0	0.289	1.03	21.8	21.2	16.64	57.54	74.17	0.76
12	6.1	67.14	43.0	0.289	1.03	21.8	21.2	16.65	57.61	74.26	0.76
						Calculated:		162.25	697.44	859.69	
						Measured:		168.22	698.88	867.10	
						Difference (g) (calc.-meas.):		−5.97	−1.44	−7.41	
						Difference (%):		−3.6	−0.2	−0.9	

By measuring the height and diameter of the discs on both twins before and after drying, it was determined that the changes in their heights were proportional to the changes in the diameter of the discs. Based on this, the proportion of the difference in the height of an individual disk in the total measured change in the height of the sample was calculated proportionately to the measured change in diameter. In this way, the volumes of all discs during drying were determined. The known relationship between the void ratio and moisture content determined the moisture content profiles during drying (Tables 1 and 2).

Table 2. Conditions of sample VU-3 after drying for 41 days.

After drying for 41 days, sample VU-3 was divided into 12 discs of equal height: 12.07 mm											
After drying, the sample was subjected to one-dimensional wetting.											
Specific gravity of solid particles: 2.72											
Relation between moisture content and void ratio: for $w > 0.408 \rightarrow e = 2.72\ w \rightarrow$ proportional shrinkage phase for $w < 0.408 \rightarrow e = 0.66\ w + 0.84 \rightarrow$ residual shrinkage phase											
VU-3		Measured		Assum. mois-ture content, w	Calculated						
Disc no.	Height of meas. point (mm)	Disc dia. (mm)	Disc volume (cm^3)		Void ratio, e	Void volume (cm^3)	Vol. of solids (cm^3)	Water mass (g)	Mass of solids (g)	Disc mass (g)	Degree of satur. S
1	138.8	66.09	41.4	0.079	0.89	19.5	21.9	4.72	59.51	64.23	0.24
2	126.7	66.45	41.9	0.130	0.93	20.1	21.7	7.67	59.12	66.79	0.38
3	114.6	66.56	42.0	0.177	0.96	20.5	21.5	10.31	58.38	68.69	0.50
4	102.6	66.86	42.4	0.215	0.98	21.0	21.4	12.49	58.16	70.64	0.59
5	90.5	67.00	42.5	0.240	1.00	21.3	21.3	13.91	57.91	71.82	0.65
6	78.4	67.13	42.7	0.259	1.01	21.5	21.2	14.97	57.77	72.74	0.70
7	66.4	67.22	42.8	0.271	1.02	21.6	21.2	15.61	57.71	73.32	0.72
8	54.3	67.31	42.9	0.279	1.02	21.7	21.2	16.09	57.71	73.80	0.74
9	42.2	67.34	43.0	0.285	1.03	21.8	21.2	16.41	57.65	74.06	0.75
10	30.2	67.27	42.9	0.289	1.03	21.8	21.1	16.60	57.45	74.05	0.76
11	18.1	67.27	42.9	0.289	1.03	21.8	21.1	16.61	57.45	74.06	0.76
12	6.0	67.22	42.8	0.289	1.03	21.7	21.1	16.58	57.37	73.94	0.76
						Calculated:		161.97	696.18	858.15	
						Measured:		168.20	699.00	867.20	
						Difference (g) (calc.-meas.):		−6.23	−2.82	−9.05	
						Difference (%):		−3.7	−0.4	−1.0	

5.2. Wetting of VU-3

After 1D drying for 41 days, the VU-3 twin was prepared for vertical one-dimensional wetting. The state of the twin, before wetting, in terms of moisture content distribution, void ratio, and material saturation, is shown in Table 2.

Before wetting, the VU-3 twin was virtually divided into 12 discs of equal height by engraving markings. It is assumed that the moisture content and void ratio profiles per depth of the sample are identical to the profiles determined on the VU-4 twin.

After engraving the marks representing the boundaries between the discs, measuring each disc's diameter, and controlling the mass of the VU-3 before wetting, the sample was placed on the prepared stand. The rubber plug was removed from the opening in the sample stand. The opening in the stand was used for air drainage, which was forced out through the sample's lower base due to the wet front's penetration. The sample was then coated with a new thin rubber membrane. A plexiglass cylinder with an outer diameter of 70 mm and a height of 32 mm was placed on top of the sample, which was to be filled with water during wetting. The membrane covered the stand, the twin, and the cylinder, and was secured by a rubber ring over the stand (Figure 6). A thin filter plate with a diameter of 36 mm and a thickness of 2 mm was placed in the center of the upper base of the twin. A filter paper is placed under the plate. The plate served as support below the dial gauge plunger.

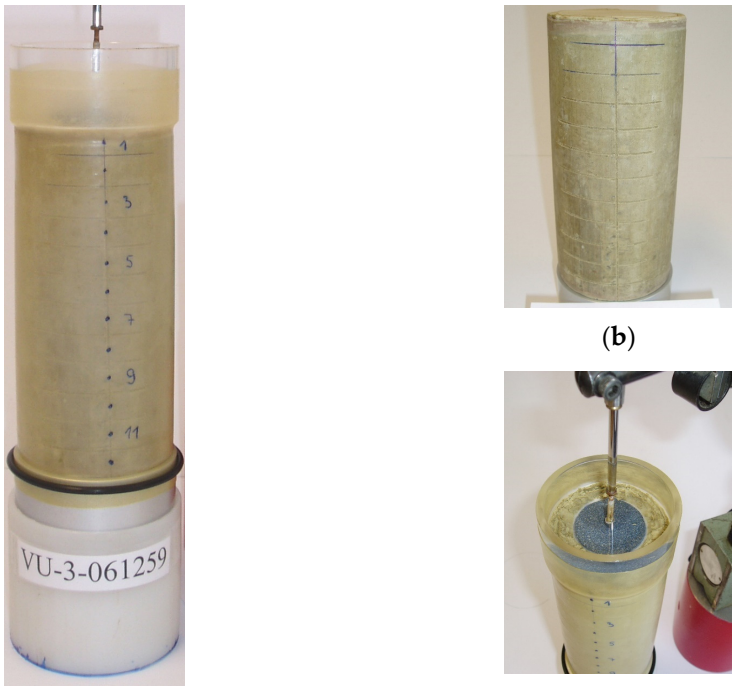

(**a**) (**b**) (**c**)

Figure 6. Preparation of VU-3 for the 1D wetting phase: (**a**) the VU-3 on the stand with the cylinder on the top; (**b**) the VU-3 without the rubber membrane with the engraved marks; (**c**) the cylinder on the top filled with water at the start of the wetting phase.

Lateral changes in the twin volume were possible since a thin, flexible rubber membrane surrounded the sample. A relatively small force of the dial gauge plunger acted on the upper surface of the twin during the wetting test. If the resistances of the thin membrane and the dial gauge plunger were neglected, the sample was in the condition of quasi-free three-dimensional swelling. Only the upper surface of the sample was exposed to wetting under the action of a column of water with an average height of h = 3 cm.

The wetting experiment, the advance of the wet front, and the changes in the total height of the sample are shown chronologically in Figure 7.

The mass of VU-3 was measured immediately before wetting and again at the end of wetting (Table 3). The difference in the mass of the sample represented the mass of the total infiltrated water in the sample. Changes in the value of the mass of the infiltrated water, which occurred during the experiment, were registered indirectly as the difference in the value of the mass of the water added (to the top of the cylinder) and the water evaporated from the cylinder into the surrounding air. The mass of evaporated water was registered with each addition of water on an auxiliary control cylinder near the sample. The cross-sectional area of the control cylinder was equal to the surface of the water above the VU-3 during a wetting test. At the end of wetting, the value of the indirectly determined mass of infiltrated water was about 3.3% lower than the actual value, which was determined as the difference between the sample masses measured at the end and beginning of wetting. Indirect or calculated values of the mass of infiltrated water were linearly corrected so that the mass of infiltrated water at the end of the experiment corresponded to the measured value.

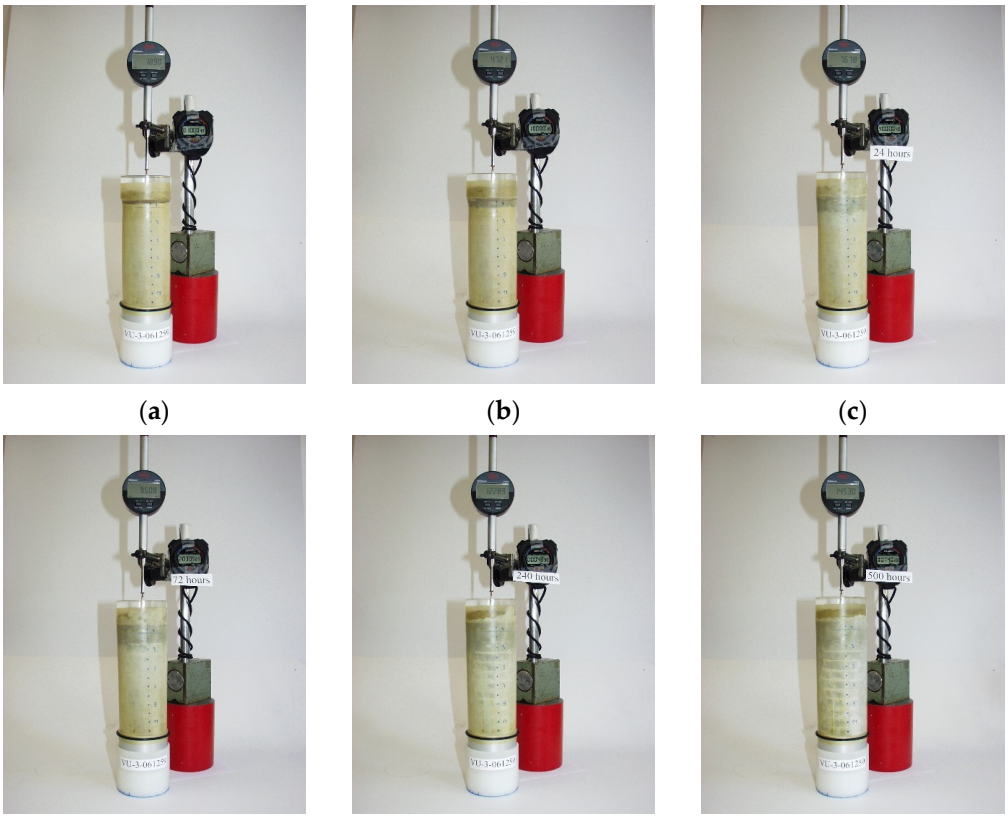

Figure 7. VU-3 at different times after the start of the wetting phase: (**a**) 10 min; (**b**) 1 h; (**c**) 24 h; (**d**) 72 h; (**e**) 240 h; (**f**) 500 h.

Figure 8 shows the curve of change in the mass of the infiltrated water and the curve of change in volume (swelling) during wetting of VU-3. Changes in the diameter of each disc were regularly measured with a calliper during the wetting experiment. Figure 9 shows the changes in the height of the VU-3 during the wetting experiment.

Wetting was maintained for three weeks. At the end of the experiment, the membrane was removed from the VU-3, and the disc diameters and total mass were measured. The heights of individual discs were calculated based on the assumption that the contribution of the change in the height of a disc in the total measured change in the height of the sample is equal to the share of its diameter change in the sum of the changes in the diameter of all discs. The correctness of this assumption was confirmed by rough control of the height of the discs at the place of the vertically engraved mark.

The sample was cut into 12 discs according to the previously engraved marks. During cutting, the discs broke into irregularly shaped pieces. The moisture content of the material from each disc was determined by drying it in an oven at 60 °C until it reached a constant mass.

The changes in the volume of individual discs during the experiment were calculated from the measured changes in the total height of the sample and the changes in the diameter of the discs. Based on the calculated volumes of the discs and the known volumes of solid particles in each disc (also determined for the moment after drying, Table 2), the profiles of the void ratio during wetting were calculated. In this way, the profiles of the void ratio (Figure 10), moisture content (Figure 11), and degree of saturation (Figure 12) of the material were determined during the wetting experiment. The state of the sample after the wetting test is shown in Table 3.

Table 3. Conditions of sample VU-3 after 21 days of 1D wetting.

After 1D wetting for 21 days, sample VU-3 was divided into 12 discs according to the previously engraved marks. During cutting, the material broke into pieces of irregular shapes. The moisture content of the material from each disc was determined by drying in a drying oven at 60 °C until it reached a constant mass. Based on the measured dimensions, the volume of each disc was determined, and the mass of solids in each disc was determined before wetting, i.e., at the end of drying.

Specific gravity of solid particles: 2.72

VU-3	Measured					Calculated					
Disc no.	Height of meas. point (mm)	Disc dia. (mm)	Disc volume (cm^3)	Moisture content, w	Void ratio, e	Void volume (cm^3)	Volume of solids (cm^3)	Water mass (g)	Mass of solids (g)	Disc mass (g)	Degree of saturation, S
1	152.3	71.10	73.8	0.840	2.38	52.0	21.9	49.99	59.51	109.50	0.96
2	135.8	71.09	57.2	0.504	1.63	35.5	21.7	29.79	59.12	88.91	0.84
3	121.8	70.96	53.6	0.475	1.50	32.1	21.5	27.71	58.38	86.08	0.86
4	108.6	70.77	50.8	0.466	1.38	29.4	21.4	27.13	58.16	85.28	0.92
5	95.7	70.73	50.6	0.463	1.38	29.3	21.3	26.83	57.91	84.74	0.92
6	82.8	70.68	50.4	0.462	1.37	29.2	21.2	26.67	57.77	84.44	0.91
7	70.0	70.45	49.9	0.461	1.35	28.6	21.2	26.59	57.71	84.30	0.93
8	57.2	70.36	49.7	0.459	1.34	28.5	21.2	26.48	57.71	84.19	0.93
9	44.4	70.24	49.4	0.458	1.33	28.2	21.2	26.39	57.65	84.04	0.93
10	31.7	69.94	48.9	0.458	1.31	27.7	21.1	26.30	57.45	83.75	0.95
11	19.0	69.73	48.5	0.458	1.30	27.4	21.1	26.28	57.45	83.73	0.96
12	6.3	69.48	48.0	0.453	1.27	26.9	21.1	25.99	57.37	83.36	0.97
						Calculated:		346.15	696.18	1042.33	
						Measured:		354.35	699.00	1053.35	
						Difference (g) (calc.-meas.):		−8.20	−2.82	−11.02	
						Difference (%):		−2.3	−0.4	−1.0	

Changes in the moisture content of each disc were interpreted based on assumed swelling curves and measured changes in volume or void ratio value. The degree of saturation of the material during wetting was calculated based on the interpreted moisture content and the measured values of the void ratio.

Based on the conceptual swelling curve (Figure 2) proposed here, i.e., the behaviour model of the representative elementary volume (REV) of the swelling material in the wetting process, the initial part of the swelling curve is, therefore, assumed to be a line with a slope equal to the value of the specific gravity of the material (e = 2.72 w; see Table 1). The VU-3 is divided into 12 discs. A swelling curve was assumed for each disc starting from the initial moisture content point on the drying curve. The curve holds a direction parallel to the line of full saturation up to the intersection with another curve parallel to the direction of the residual drying phase (k_{rez} = 0.66; see Table 1) and is laid through the point of final moisture content (after wetting). The assumed swelling curves are shown in Figure 13.

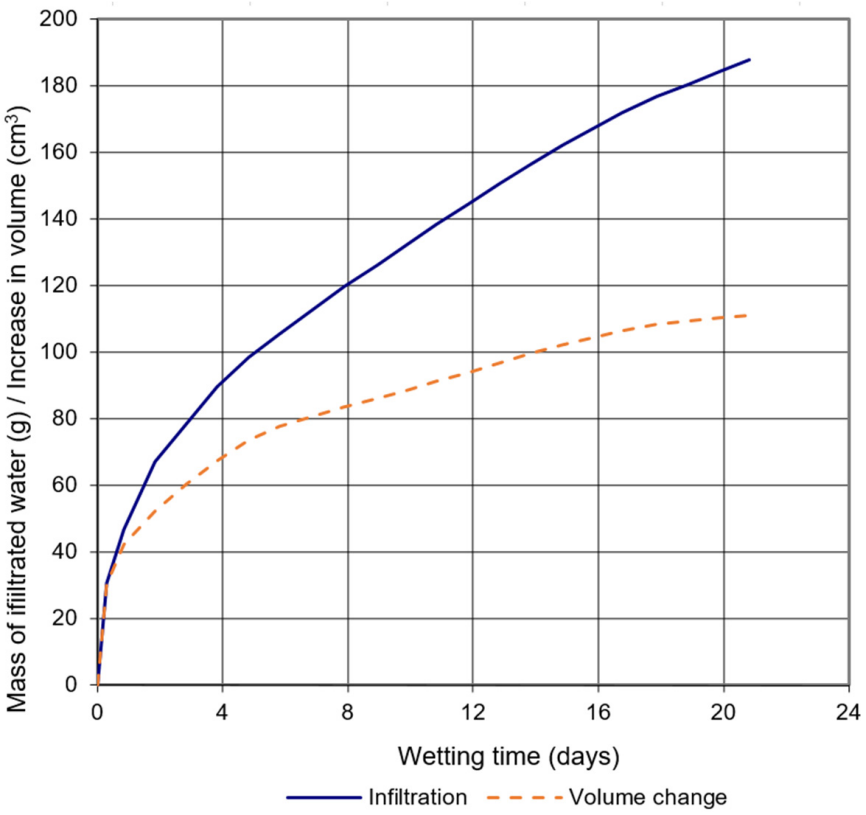

Figure 8. Changes in the mass of infiltrated water and changes in the sample volume during the wetting experiment.

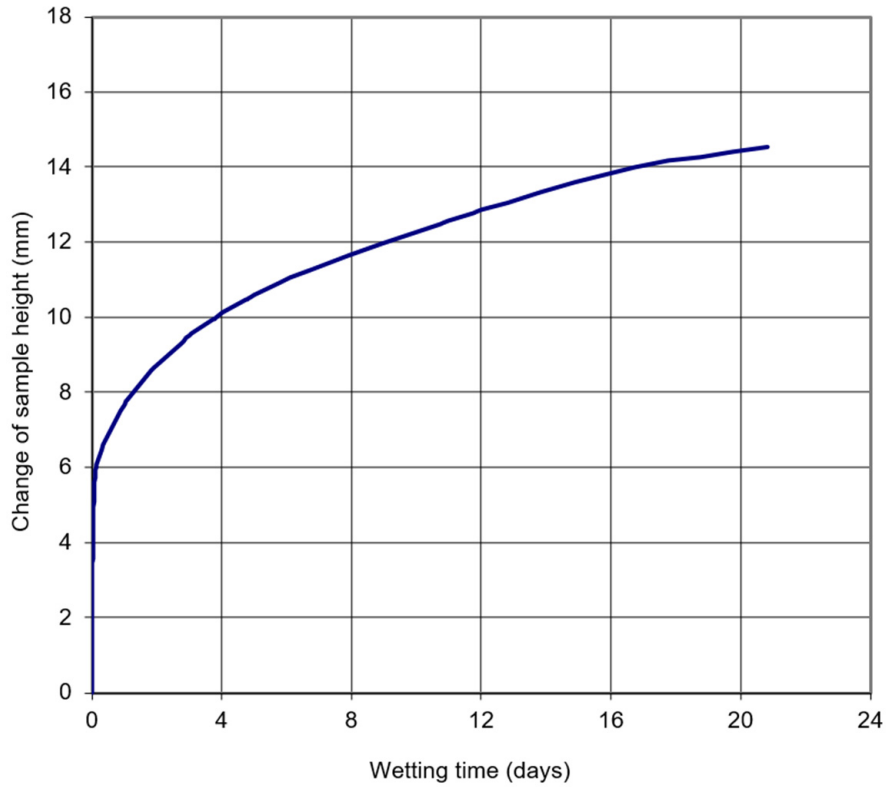

Figure 9. Changes in the height of the VU-3 during the wetting experiment.

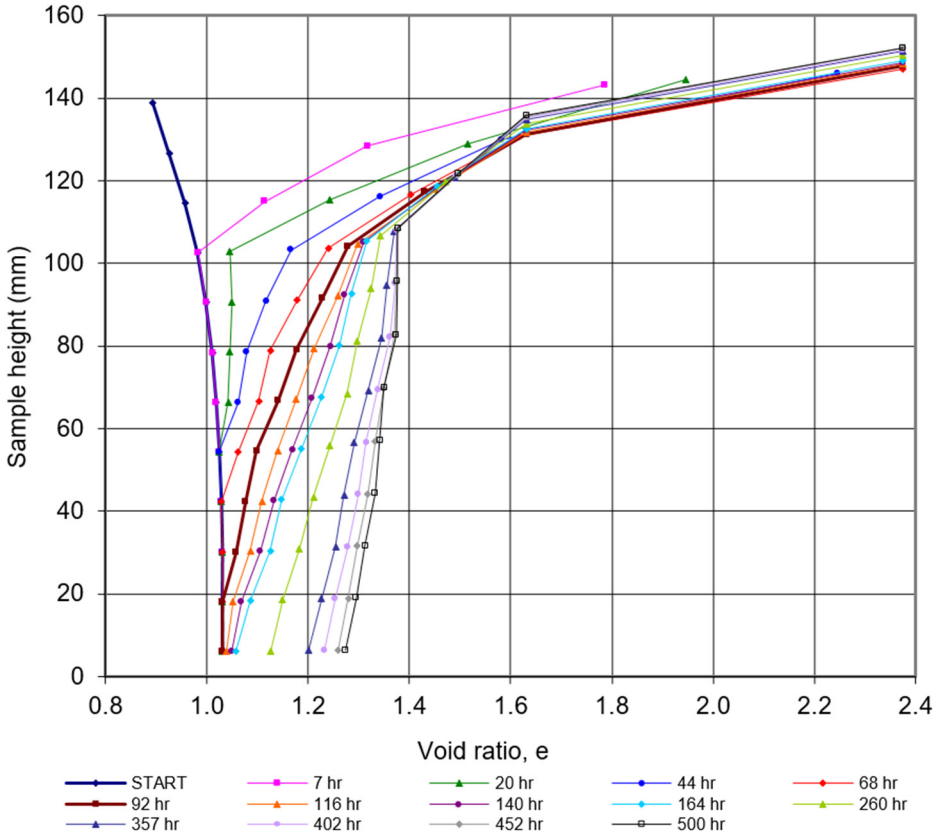

Figure 10. Profiles of the void ratio in the wetting experiment of VU-3.

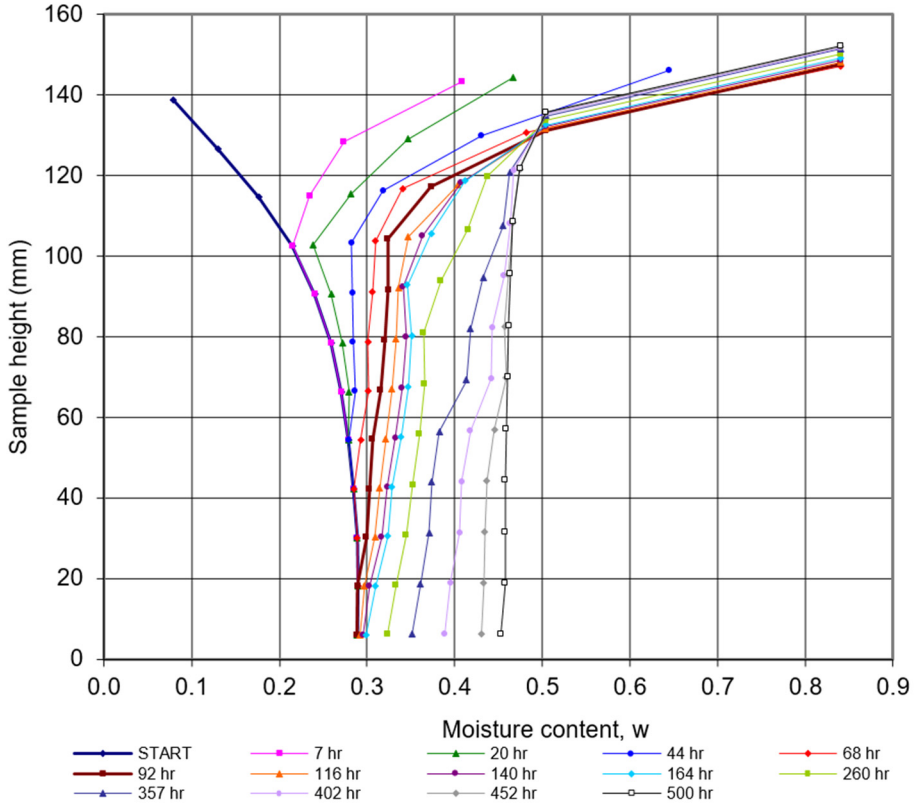

Figure 11. Moisture content profiles in the wetting experiment of VU-3.

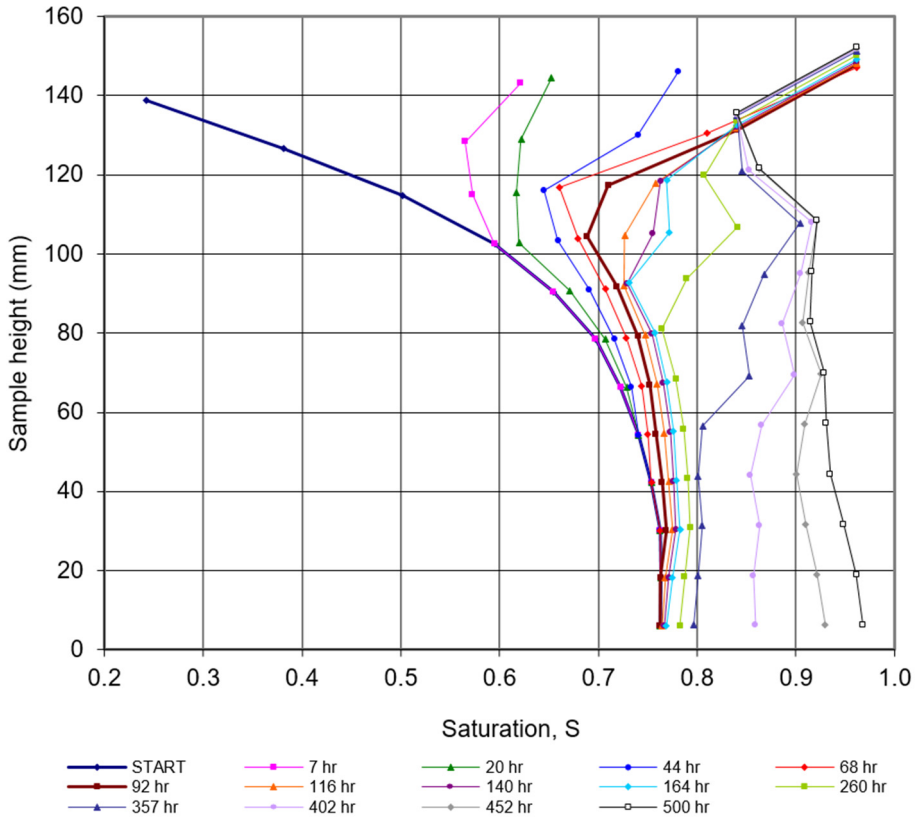

Figure 12. Degree of saturation profiles in the wetting experiment of VU-3.

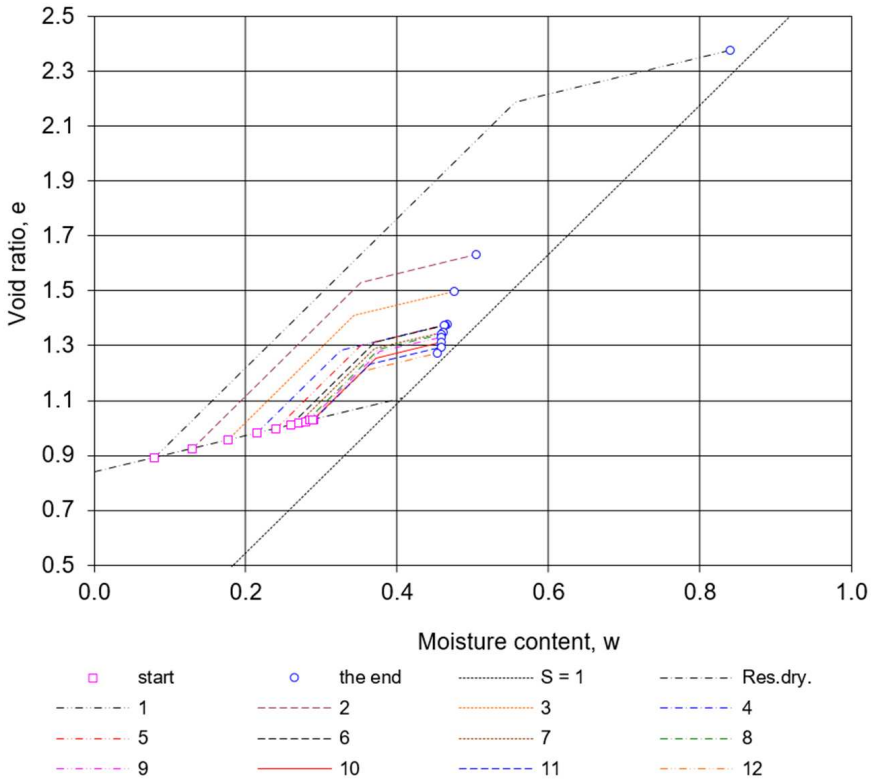

Figure 13. Assumed swelling curves in the wetting experiment of VU-3.

6. Discussion

By consolidating the paste in a tall cylinder according to the procedure developed here, two identical reconstituted samples (VU-3 and VU-4) were prepared, the so-called "twins". The twins were simultaneously subjected to one-dimensional drying in the laboratory, side by side, under identical environmental conditions. The samples' mass, height, and diameter were measured during drying. After drying, the VU-4 sample was cut into 12 discs of equal height to measure the moisture content distribution along the depth of the sample. The behaviour of twins during drying in terms of change in mass and volume was similar and almost identical.

After drying, the second twin (VU-3) was subjected to the effect of a constant column of water, i.e., one-dimensional wetting. Based on the measured moisture content profile in the first twin, an identical profile in the second twin was assumed. The VU-3 was virtually divided into 12 discs of equal height by engraved markings. Lateral volume changes during wetting were enabled because a flexible thin rubber membrane surrounded the sample.

The wetting experiment lasted three weeks. The swelling was dynamic and intense at the very beginning of wetting. In the first hour, the first disc was affected by wetting, and approximately one-third of the sample's total vertical deformation was achieved in that short time. The wet front affected the first three discs in the first 7 h of the experiment. After two days, about 50% of the total change in volume was achieved, and after eight days from the start of wetting, about 75% of the total change in volume was achieved.

At the end of the wetting experiment, the sample was cut into 12 discs, and the moisture content of each disc was determined. The material of the first disc, at the very top, behaved differently from the rest of the sample. The separation of thin layers of material was observed on the sample's surface in contact with water (Figure 14). However, this happened only in the shallow surface part, about 5 mm into the depth of the material. The "shells" of the separated material in the water disintegrated (dispersed) into smaller particles very quickly, within 1 h (Figure 14). Therefore, it is to be assumed that at the top of the sample, due to the disintegration of the structure of the swelling material, the osmotic action in the microdomain did not encounter obstruction in the form of matrix action from the macrodomain, that is, the balance between these conflicting actions was not established here. According to the concept presented here, the swelling in the tertiary phase stops only after the dissipation of the suction in the micropores or after the eventual establishment of a balance between the osmotic effect and the forces that resist the volume change.

The lower-lying material, although significantly desaturated, did not disintegrate like the surface material. However, with the advance of the moist front, the air that slowed down the wetting was pushed and trapped there, and this is clearly shown by the data on the degree of saturation of the material after the wetting experiment, which was the lowest in the second disc below the top (S = 84%, Table 3). At the end of the wetting experiment, the saturations at the top and bottom of the sample were very high, at over 95%.

Figure 8 shows the curve of the mass change in the infiltrated water and the curve of the sample volume increase during the wetting time. The applied techniques for measuring the mass of infiltrated water and changes in the sample volume were unfortunately too slow, insufficient, and unsuitable for a better analysis of the very beginning of the wetting process when changes in moisture content and volume occur very quickly. Despite this, based on the collected data, it is still possible to conclude that at the beginning of wetting, the ratio of the mass of infiltrated water and the volume change was approximately 1:1. Further changes in volume and moisture content after that dynamic start were much slower. It was possible to monitor them satisfactorily with the applied measurement techniques.

A reinterpretation of the results of measurements performed using a synchrotron dual X-ray source, which was performed and published by Garnier et al. [23], was also carried out here. The reinterpretation results shown in Figure 3 confirm the hypothesis about the existence of primary and secondary swelling phases. Likewise, Garnier et al. [23] described the phenomenon of material dispersion at the top of the Vertisol sample, which was also observed and explained here.

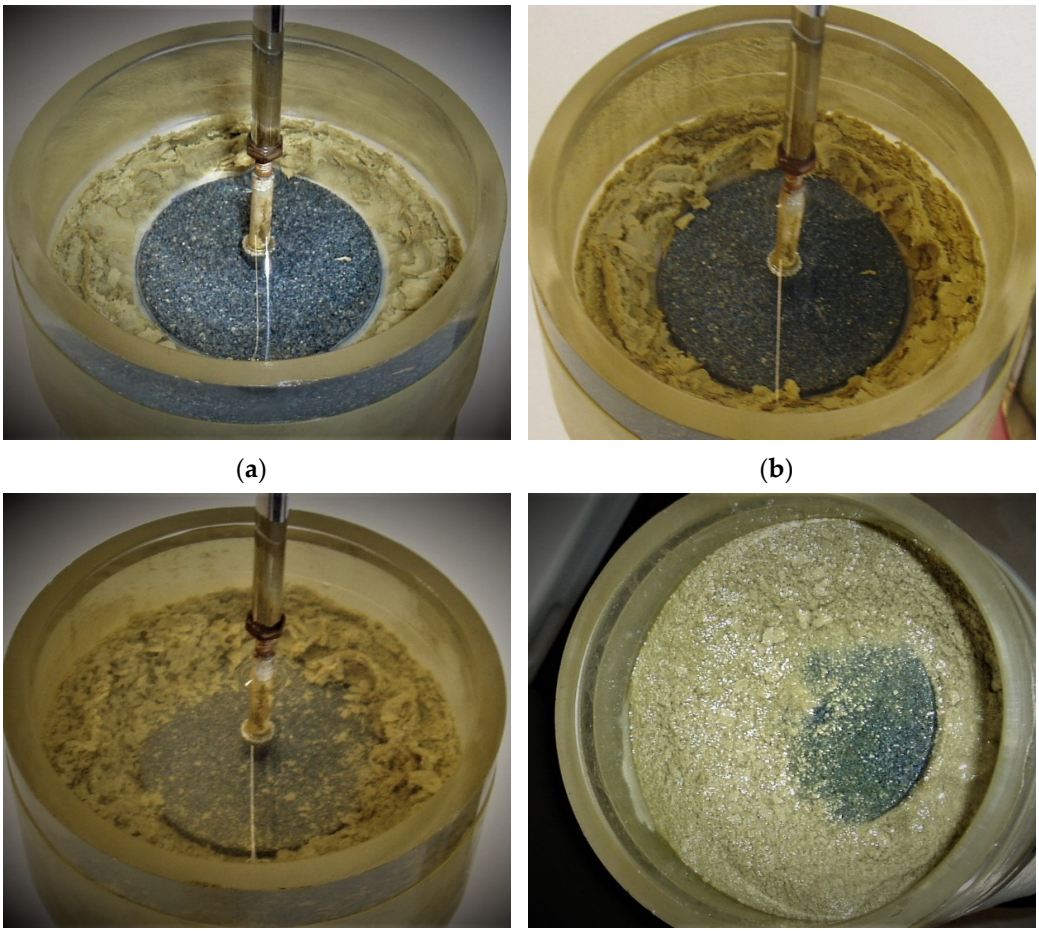

Figure 14. Top surface of VU-3 at different times after the start of the wetting phase: (**a**) 1 min; (**b**) 3 min; (**c**) 60 min; (**d**) 21 days.

Based on the observed behaviour of the swelling material, swelling curves were assumed (Figure 13), wherein in the initial primary phase, the change in material volume corresponds to the volume of infiltrated water. In the secondary phase, the slope of the curve corresponds to the slope of the residual part of the shrinkage curve. Changes in moisture content by sample depth and volume were interpreted using measured changes in void ratio and assumed swelling curves. The interpretation of moisture content changes based on assumed swelling curves qualitatively and quantitatively shows a relatively good agreement with the measured data and control of the sample mass (Figure 15). Recorded deviations between the calculated and measured curves, which can be seen in Figure 15, are, to the greatest extent, a consequence of the relatively coarse discretization of the sample on 12 discs only and also the errors present in the volume measurements.

Finally, the achieved results undoubtedly indicate that the concept of the swelling model is good and that it can be used to realistically interpret changes in the moisture content of the swelling material into changes in volume.

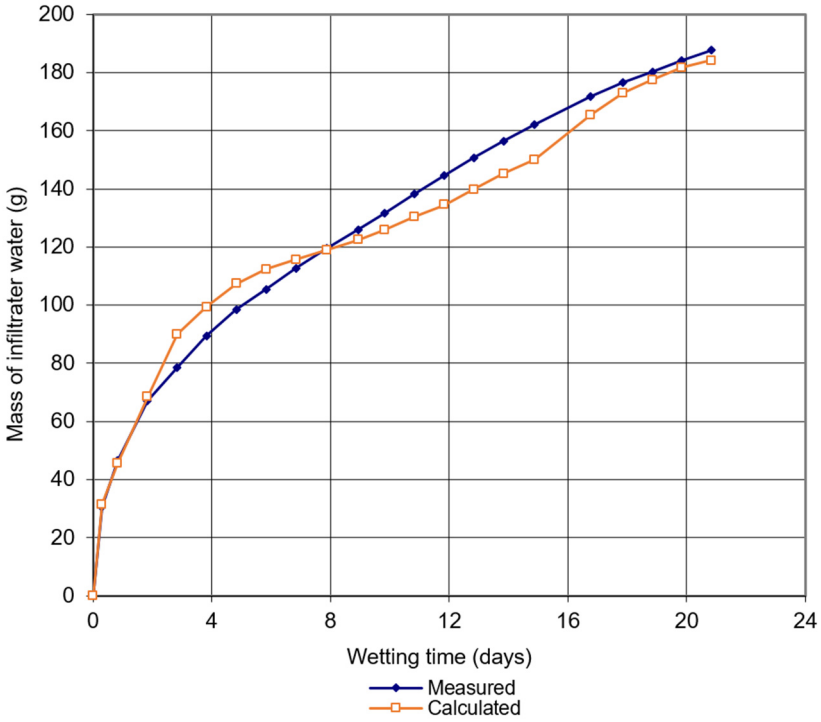

Figure 15. Measured and calculated curves of infiltrated water mass in the wetting of VU-3.

7. Conclusions

An original swelling model was proposed to interpret moisture content profiles obtained in the wetting experiment of swelling material, which was developed on the hypothesis that parts of the same swelling material that differ in moisture content at the beginning of wetting will have separate swelling curves. The proposed model predicts primary and secondary phases of swelling and assumes that the swelling curves, and their parts by phase, are approximately parallel.

The results of the wetting experiment of desaturated swelling material showed that the initial part of the swelling curve has a significantly higher slope (primary phase) than the residual part of the shrinkage curve and that the assumption that the volume increase in this phase corresponds approximately to the volume of infiltrated water (1:1) is realistic. After such an initial part, changes in volume as the wetting process progresses become smaller. After a certain increase in moisture content, the slope of the swelling curve is equal to the slope of the residual part of the shrinkage curve (secondary phase). The proposed model interpreted the data obtained in the wetting experiment and gave a realistic picture of swelling, confirming the set hypothesis.

For the implementation of the proposed swelling model, it is necessary to determine the void ratio corresponding to the material's shrinkage limit and the shrinkage curve's slope in the residual phase through drying experiments of the swelling material.

Regarding the tertiary phase, the applied techniques were too slow for a better analysis, and the proposed model needs further development for that phase.

The data collected through this research will be used in the next step for calibrating the numerical model of drying and wetting of the swelling material and for further research on the hysteresis between drying and wetting.

Author Contributions: Conceptualization, B.K.; methodology, B.K.; software, B.K. and J.J.; validation, B.K., N.Š.C., J.J. and I.V.; formal analysis, B.K.; investigation, B.K.; resources, B.K.; data curation, B.K.; writing—original draft preparation, B.K, N.Š.C. and J.J.; writing—review and editing, B.K, N.Š.C. and J.J.; visualization, B.K. and J.J.; supervision, B.K. and N.Š.C.; project administration, B.K.; funding acquisition, B.K. All authors have read and agreed to the published version of the manuscript.

Funding: This research received no external funding.

Data Availability Statement: The data supporting the results of this research work have been reported in this manuscript.

Acknowledgments: Authors convey gratitude to the reviewers and editors for valuable comments and suggestions that greatly improved the manuscript.

Conflicts of Interest: The authors declare no conflict of interest.

References

1. Grob, H. Swelling and Heave in Swiss tunnels. *Bull. Int. Assoc. Eng. Geol.* **1976**, *13*, 55–60. [CrossRef]
2. Einstein, H.H. Tunnelling in swelling rock. *Undergr. Space* **1979**, *4*, 51–61.
3. Houston, S.L.; Dye, H.B.; Zapata, C.E.; Walsh, K.D.; Houston, W.N. Study of expansive soils and residential foundations on expansive soils in Arizona. *J. Od Perform. Constr. Facil.* **2011**, *25*, 31–44. [CrossRef]
4. Jones, L.D.; Jefferson, I. Expansive soils. In *ICE Manual of Geotechnical Engineering, Volume 1 Geotechnical Engineering Principles, Problematic Soils and Site Investigation*; Burland, J., Chapman, T., Skinner, H., Brown, M., Eds.; ICE Publishing: London, UK, 2012; pp. 413–441.
5. Harrison, A.M.; Plim, J.; Harrison, M.; Jones, L.D.; Culshaw, M.G. The relationship between shrink–swell occurrence and climate in south-east England. *Proc. Geol. Assoc.* **2012**, *123*, 556–575. [CrossRef]
6. Zheng, J.L.; Zheng, R.; Yang, H.P. Highway subgrade construction in expansive soil areas. *J. Mater. Civ. Eng.* **2009**, *21*, 154–162. [CrossRef]
7. Bell, F.G.; Culshaw, M.G. Problem Soils: A review from a British perspective. In *Problematic Soils Symposium*; Jefferson, I., Murray, E.J., Faragher, E., Fleming, P.R., Eds.; Thomas Telford Publishing: Nottingham, UK, 2001; pp. 1–35.
8. Driscoll, R.M.C.; Chown, R. Shrinking and swelling of clays. In *Problematic Soils Symposium*; Jefferson, I., Murray, E.J., Faragher, E., Fleming, P.R., Eds.; Thomas Telford Publishing: Nottingham, UK, 2001; pp. 53–66.
9. Nelson, J.D.; Miller, D.J. *Expansive Soils: Problems and Practice in Foundation and Pavement Engineering*, 1st ed.; John Wiley and Sons Inc.: New York, NY, USA, 1992.
10. Radevsky, R. Expansive clay problems–how are they dealt with outside the US? Expansive clay soils and vegetative influence on shallow foundations. *ASCE Geotech. Spec. Publ.* **2001**, *115*, 172–191.
11. Vrkljan, I.; Kavur, B.; Znidarčić, D. Influence of desiccation on swelling behavior of initially saturated swelling rocks. In Proceedings of the XIIIth Danube-European Conference on Geotechnical Engineering, Ljubljana, Slovenia, 29 May–1 June 2006; Volume 2, pp. 159–164.
12. Vrkljan, I. Bujanje Stijena i Njegov Utjecaj na Podzemne Objekte/Rock Swelling and Its Impact on Underground Construction. Ph.D. Thesis, Faculty of Civil Engineering, University of Zagreb, Zagreb, Croatia, 1997.
13. Kavur, B.; Vrkljan, I.; Kovačević Zelić, B. Procjena hidrauličkih značajki nezasićenog ekspanzivnog tla/Analysis of hydraulic properties of unsaturated expansive soil. *Građevinar J. Assoc. Civ. Eng. (HSGI)* **2011**, *3*, 245–253.
14. Znidarčić, D.; Schiffman, R.L.; Pane, V.; Croce, P.; Ko, H.Y.; Olsen, H.W. The Theory of One-Dimensional Consolidation of Saturated Clays: V, Constant Rate of Deformation Testing and Analysis. *Geotechnique* **1986**, *36*, 227–237. [CrossRef]
15. Znidarčić, D.; Illangasekare, T.; Manna, M. Laboratory testing and parameter estimation for two-phase flow problems. *ASCE Geotech. Spec. Publ.* **1991**, *27*, 1089–1099.
16. Znidarčić, D.; Hwang, C.; Bicalho, K.V. Experimental determination of hydraulic characteristics for unsaturated soils. In *Unsaturated Soils*; CRC Press: Boca Raton, FL, USA, 2021; Volume 3, pp. 1137–1141.
17. Abu-Hejleh, A.N.; Znidarčić, D.; Illangasekare, T.H. Permeability Determination for Unsaturated Soils. *Unsaturated Soils, ASCE Geotech. Spec. Publ.* **1993**, *39*, 163–174.
18. Abu-Hejleh, A.N.; Znidarčić, D. Consolidation Characteristics of Phosphatic Clays. *ASCE J. Geotech. Eng.* **1996**, *122*, 295–301. [CrossRef]
19. Bicalho, K.V. Modeling Water Flow in an Unsaturated Compacted Soil. Ph.D. Thesis, University of Colorado, Boulder, CO, USA, 1999.
20. Hwang, C. Determination of Material Functions for Unsaturated Flow. Ph.D. Thesis, University of Colorado, Boulder, CO, USA, 2002.
21. Yao, D.T.C.; Oliveira-Filho, W.L.; Cai, X.C.; Znidarčić, D. Numerical solution for consolidation and desiccation of soft soils. *Int. J. Numer. Anal. Methods Geomech.* **2002**, *26*, 139–161. [CrossRef]
22. Onyelowe, K.C.; Mojtahedi, F.F.; Azizi, S.; Mahdi, H.A.; Sujatha, E.R.; Ebid, A.M.; Darzi, A.G.; Aneke, F.I. Innovative Overview of SWRC Application in Modeling Geotechnical Engineering Problems. *Designs* **2022**, *6*, 69. [CrossRef]
23. Garnier, P.; Angulo-Jaramillo, R.; DiCarlo, D.A.; Bauters, T.W.J.; Darnault, C.J.G.; Steenhuis, T.S.; Parlange, J.Y.; Baveye, P. Dual-energy synchrotron X ray measurements of rapid soil density and water content changes in swelling soils during infiltration. *Water Resour. Res.* **1998**, *34*, 2837–2842. [CrossRef]
24. Kavur, B. Utjecaj Sušenja na Ponašanje Bubrive Stijene/Influence of Drying on Swelling Rock Behaviour. Ph.D. Thesis, Faculty of Mining, Geology and Petroleum Engineering, University of Zagreb, Zagreb, Croatia, 2009.

25. Fredlund, D.G.; Xing, A. Equations for the soil-water characteristic curve. *Can. Geotech. J.* **1994**, *31*, 521–532. [CrossRef]
26. Fredlund, D.G.; Rahardjo, H. *Soil Mechanics for Unsaturated Soils*, 1st ed.; John Wiley and Sons Inc.: New York, NY, USA, 1993.
27. Peng, X.; Horn, R. Modelling soil shrinkage curve across a wide range of soil types. *Soil Sci. Soc. Am. J.* **2005**, *69*, 584–592. [CrossRef]
28. Vrkljan, I.; Kavur, B. Some problems of swelling in geotechnical practice–influence of saturation on the behavior of argillaceous swelling rock (invited lecture). In Proceedings of the 5th Symposium of the Macedonian Association for Geotechnics, Ohrid, Macedonia, 23–25 June 2022; pp. 144–159.
29. Smiles, D.E. Hydrology of swelling soils: A review. *Aust. J. Soil Res.* **2000**, *38*, 501–521. [CrossRef]
30. McGarry, D.; Malafant, K.W.J. The analysis of volume change in unconfined units of soil. *Soil Sci. Soc. Am. J.* **1987**, *51*, 290–297. [CrossRef]
31. Raats, P.A.C. Flow of Water in Rigid and Non-Rigid, Saturated and Unsaturated Soils. In *Modeling and Mechanics of Granular and Porous Materials. Modeling and Simulation in Science, Engineering and Technology*, 1st ed.; Capriz, G., Ghionna, V.N., Giovine, P., Eds.; Birkhäuser: Boston, MA, USA, 2002.
32. Talsma, T. A note on the shrinkage behaviour of a clay paste under various loads. *Aust. J. Soil Res.* **1977**, *15*, 275–277. [CrossRef]
33. Tariq, A.R.; Durnford, D.S. Analytical volume change model for swelling clay soils. *Soil Sci. Soc. Am. J.* **1993**, *57*, 1183–1187. [CrossRef]
34. Braudeau, E.; Costantini, J.M.; Bellier, G.; Colleuille, H. New device and method for soil shrinkage curve measurement and characterization. *Soil Sci. Soc. Am. J.* **1999**, *63*, 525–535. [CrossRef]
35. Groenevelt, P.H.; Grant, C.D. Re-evaluation of the structural properties of some British swelling soils. *Eur. J. Soil Sci.* **2001**, *52*, 469–477. [CrossRef]
36. Boivin, P.; Garnier, P.; Tessier, D. Relationship between clay content, clay type and shrinkage properties of soil samples. *Soil Sci. Soc. Am. J.* **2004**, *68*, 1145–1153. [CrossRef]
37. Puppala, A.J.; Manosuthikij, T.; Chittoori, B.C.S. Swell and shrinkage characterizations of unsaturated expansive clays from Texas. *Eng. Geol.* **2013**, *164*, 187–194. [CrossRef]
38. Lu, N.; Dong, Y. Correlation between soil-shrinkage curve and water-retention characteristics. *J. Geotech. Geoenviron. Eng.* **2017**, *143*, 1–11. [CrossRef]
39. Li, L.; Zhang, X. A New Approach to Measure Soil Shrinkage Curve. *Geotech. Test. J.* **2018**, *42*, 1–18. [CrossRef]
40. Khan, S.; Ivoke, J.; Nobahar, M. Coupled Effect of Wet-Dry Cycles and Rainfall on Highway Slope Made of Yazoo Clay. *Geosciences* **2019**, *9*, 341. [CrossRef]
41. Ahmed, A.; Hossain, M.S.; Pandey, P.; Sapkota, A.; Thian, B. Deformation Modeling of Flexible Pavement in Expansive Subgrade in Texas. *Geosciences* **2019**, *9*, 446. [CrossRef]
42. Shrestha, A.; Jotisankasa, A.; Chaiprakaikeow, S.; Pramusandi, S.; Soralump, S.; Nishimura, S. Determining Shrinkage Cracks Based on the Small-Strain Shear Modulus–Suction Relationship. *Geosciences* **2019**, *9*, 362. [CrossRef]
43. Vail, M.; Zhu, C.; Tang, C.-S.; Anderson, L.; Moroski, M.; Montalbo-Lomboy, M.T. Desiccation Cracking Behavior of MICP-Treated Bentonite. *Geosciences* **2019**, *9*, 385. [CrossRef]
44. Menon, S.; Song, X. Coupled Analysis of Desiccation Cracking in Unsaturated Soils through a Non-Local Mathematical Formulation. *Geosciences* **2019**, *9*, 428. [CrossRef]
45. Qi, W.; Wang, C.; Zhang, Z.; Huang, M.; Xu, J. Experimental Investigation on the Impact of Drying–Wetting Cycles on the Shrink–Swell Behavior of Clay Loam in Farmland. *Agriculture* **2022**, *12*, 245. [CrossRef]
46. Ivoke, J.; Khan, M.S.; Nobahar, M. Unsaturated Hydraulic Conductivity Variation of Expansive Yazoo Clay with Wet-Dry Cycles. *Transp. Res. Rec.* **2021**, *2675*, 629–641. [CrossRef]
47. Luo, Y.; Zhang, J.; Zhou, Z.; Aguilar-Lopez, J.P.; Greco, R.; Bogaard, T. Effects of dynamic changes of desiccation cracks on preferential flow: Experimental investigation and numerical modeling. *Hydrol. Earth Syst. Sci.* **2023**, *27*, 783–808. [CrossRef]
48. Meshram, K.; Singh, N.; Jain, P.K. Estimation of swelling characteristics of expansive soils with influence of clay mineralogy. *Acta Agric. Scand. Sect. B—Soil Plant Sci.* **2021**, *71*, 202–207. [CrossRef]
49. Rao, B.H.; Reddy, P.S.; Mohanty, B. Combined effect of mineralogical and chemical parameters on swelling behaviour of expansive soils. *Sci Rep.* **2021**, *11*, 16562. [CrossRef] [PubMed]
50. Garnier, P.; Perrier, E.; Angulo Jaramillo, R.; Baveye, P. Numerical model of 3-dimensional anisotropic deformation and 1-dimensional water flow in swelling soils. *Soil Sci.* **1997**, *162*, 410–420. [CrossRef]
51. Kim, D.J.; Jaramilo, R.A.; Vauclin, M.; Feyen, J.; Choi, S.I. Modeling of soil deformation and water flow in a swelling soil. *Geoderma* **1999**, *92*, 217–238. [CrossRef]
52. Bronswijk, J.J.B. Modeling of water balance, cracking and subsidence of clay soils. *J. Hydrol.* **1988**, *97*, 199–212. [CrossRef]
53. Bronswijk, J.J.B. Shrinkage geometry of a heavy clay soil at various stresses. *Soil Sci. Soc. Am. J.* **1990**, *54*, 1500–1502. [CrossRef]
54. Bronswijk, J.J.B.; Evers-Vermeer, J.J. Shrinkage of Dutch clay soil aggregates. *Neth. J. Agric. Sci.* **1990**, *38*, 175–194. [CrossRef]
55. Kim, D.J.; Vereecken, H.; Feyen, J.; Boels, D.; Bronswijk, J.J.B. On the characterization of properties of an unripe marine clay soil in relation to physical ripening. *Soil Sci.* **1992**, *153*, 471–481. [CrossRef]
56. Kim, D.J.; Vereecken, H.; Feyen, J.; Vanclooster, M.; Stroosnijder, L. A numerical model of water movement and soil deformation in a ripening marine clay soil. *Model. Geo Biosph. Process.* **1992**, *1*, 185–203.

57. Garnier, P.; Rieu, M.; Boivin, P.; Vauclin, M.; Baveye, P. Determining the hydraulic properties of a swelling soil from a transient evaporation experiment. *Soil Sci. Soc. Am. J.* **1997**, *61*, 1555–1563. [CrossRef]
58. Angulo-Jaramillo, R. Caracterisation Hydrodynamique de Sols Deformables Partiellement Satures: Etude Experimentale à L'aide de la Spectrome´Trie Gamma Double Source. Ph.D. Thesis, Institut National Polytechnique de Grenoble-INPG, Grenoble, France, 1989.
59. Barataud, F.; Stemmelen, D.; Moyne, C. Identification of the hydraulic diffusivity of a soil by inverse method with dual-energy gamma ray attenuation measurements. In *Parameter Identification and Inverse Problems in Hydrology, Geology and Ecology*; Gottlieb, J., Du Chateau, P., Eds.; Kluwer Academic Publisher: Norwell, MA, USA, 1996; pp. 123–132.
60. Fredlund, D.; Fredlund, M. Application of 'Estimation Procedures' in Unsaturated Soil Mechanics. *Geosciences* **2020**, *10*, 364. [CrossRef]
61. Sadeghi, H.; Golaghaei Darzi, A. A review of different approaches to analytical modeling of soil-water retention curves. *Sharif J. Civ. Eng.* **2021**, *37*, 111–123.
62. Al-Mahbashi, A.M.; Elkady, T.Y.; Al-Shamrani, M.A. Hysteresis soil-water characteristic curves of highly expansive clay. *Eur. J. Environ. Civ. Eng.* **2018**, *22*, 1041–1059. [CrossRef]
63. Dong, Y.; Lu, N. Measurement of suction-stress characteristic curve under drying and wetting conditions. *Geotech. Test. J.* **2017**, *40*, 107–121. [CrossRef]
64. Burton, G.J.; Pineda, J.A.; Sheng, D.; Airey, D. Microstructural changes of an undisturbed, reconstituted and compacted high plasticity clay subjected to wetting and drying. *Eng. Geol.* **2015**, *193*, 363–373. [CrossRef]
65. Yong, R.N. Soil suction and soil-water potentials in swelling clays in engineered clay barriers. *Eng. Geol.* **1999**, *54*, 3–13. [CrossRef]
66. Kavur, B.; Vrkljan, I.; Znidarčić, D. Prediction of Rock Swelling Behaviour. In Proceedings of the Sri Lankan Geotechnical Society's First International Conference on Soil & Rock Engineering, Colombo, Sri Lanka, 6–12 August 2007.